

# FECAM: Frequency Enhanced Channel Attention Mechanism for Time Series Forecasting

Maowei Jiang<sup>†</sup>  
Shenyang Institute of Automation,  
Chinese Academy of Sciences  
Shenyang, China  
University of Chinese Academy of  
Sciences  
Beijing, China  
jiangmaowei@sia.cn

Pengyu Zeng<sup>†</sup>  
Shenyang Institute of Automation,  
Chinese Academy of Sciences  
Shenyang, China  
University of Chinese Academy of  
Sciences  
Beijing, China  
zengpengyu@sia.cn

Kai Wang<sup>\*</sup>  
Shenyang Institute of Automation,  
Chinese Academy of Sciences  
Shenyang, China  
wangkai@sia.cn

Huan Liu  
Shenyang Institute of Automation,  
Chinese Academy of Sciences  
Shenyang, China  
liuhuan@sia.cn

Wenbo Chen  
Shenyang Institute of Automation,  
Chinese Academy of Sciences  
Shenyang, China  
University of Chinese Academy of  
Sciences  
Beijing, China  
chenwenbo@sia.cn

Haoran Liu  
Shenyang Institute of Automation,  
Chinese Academy of Sciences  
Shenyang, China  
University of Chinese Academy of  
Sciences  
Beijing, China  
liuhaoran@sia.cn

## ABSTRACT

Time series forecasting is a long-standing challenge due to the real-world information is in various scenario (e.g., energy, weather, traffic, economics, earthquake warning). However some mainstream forecasting model forecasting result is derailed dramatically from ground truth. we believe it's the reason that models' lacking ability of capturing frequency information which richly contains in real world datasets. At present, the mainstream frequency information extraction methods are Fourier transform(FT) based. However, use of FT is problematic due to Gibbs phenomenon. If the values on both sides of sequences differ significantly, oscillatory approximations are observed around both sides and high frequency noise will be introduced. Therefore We propose a novel frequency enhanced channel attention that adaptively modelling frequency interdependencies between channels based on Discrete Cosine Transform which would intrinsically avoid high frequency noise caused by problematic periodicity during Fourier Transform, which is defined as Gibbs Phenomenon. We show that this network generalize extremely effectively across six real-world datasets and achieve state-of-the-art performance, we further demonstrate that frequency enhanced channel attention mechanism module can be flexibly applied to different networks. This module can improve the prediction ability of existing mainstream networks, which reduces **35.99%** MSE on LSTM, **10.01%** on Reformer, **8.71%** on Informer, **8.29%** on Autoformer, **8.06%** on Transformer, etc., at a slight computational cost, with just a few line of code. Our codes and data are available at <https://github.com/Zero-coder/FECAM>.

## PVLDB Reference Format:

<sup>†</sup>These authors contributed equally to this work.  
<sup>\*</sup>Corresponding author.

Maowei Jiang<sup>†</sup>, Pengyu Zeng<sup>†</sup>, Kai Wang<sup>\*</sup>, Huan Liu, Wenbo Chen, and Haoran Liu. FECAM: Frequency Enhanced Channel Attention Mechanism for Time Series Forecasting. PVLDB, 14(1): XXX-XXX, 2020. doi:XX.XX/XXX.XX

## PVLDB Artifact Availability:

The source code, data, and/or other artifacts have been made available at <https://github.com/Zero-coder/FECAM>.

## 1 INTRODUCTION

Time series forecasting (TSF) enables decision-making with the estimated future evolution of metrics or events, thereby playing a crucial role in various scientific and engineering fields such as weather forecasting [11, 13, 30], estimation of future illness cases [10, 16, 31], energy consumption management [32, 36, 37, 44], traffic flow [24, 39, 45, 46], and financial investment [2, 3, 7, 41], to name a few.

With the growing data availability and computing power in recent years, it is shown that deep learning-based TSF methods can achieve much better prediction performance than traditional approaches [21].

In recent year, Transformers [35] have achieved progressive breakthrough on extensive areas [5, 6, 8, 23]. Especially in time series forecasting, credited to their stacked structure and the capability of attention mechanisms, Transformers [18, 35, 47] can naturally capture the temporal dependencies among time points, thereby fitting the series forecasting task perfectly.

This work is licensed under the Creative Commons BY-NC-ND 4.0 International License. Visit <https://creativecommons.org/licenses/by-nc-nd/4.0/> to view a copy of this license. For any use beyond those covered by this license, obtain permission by emailing [info@vldb.org](mailto:info@vldb.org). Copyright is held by the owner/author(s). Publication rights licensed to the VLDB Endowment.

Proceedings of the VLDB Endowment, Vol. 14, No. 1 ISSN 2150-8097.  
doi:XX.XX/XXX.XX

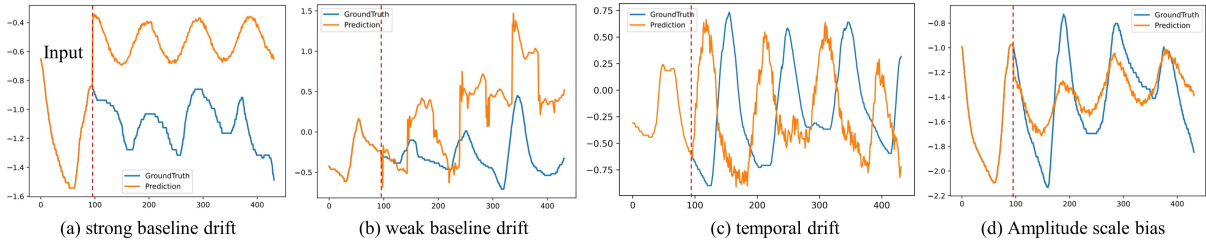


**Figure 1: The discrepancy between ground truth and forecasting output on real-world dataset ETm2,(a) is from the vanilla LSTM,(b)is from vanilla Informer(c)is from vanilla transformer (d)is from vanilla autoformer.**

Despite the promising results of TSF methods, we found that the prediction of those methods, like transformers and LSTM is way derailed from the distribution of the ground truth of datasets, such as baseline drift in Fig.1(a) and temporal drift in Fig.1(c), we believe it's the reason that models' lacking ability of capturing frequency information which richly contains in real world datasets(Fig.2). Therefore, the thing is that there still have room for improvement for these TSF mainstream methods to exploiting the natural property of time series data what we call frequency during modeling.

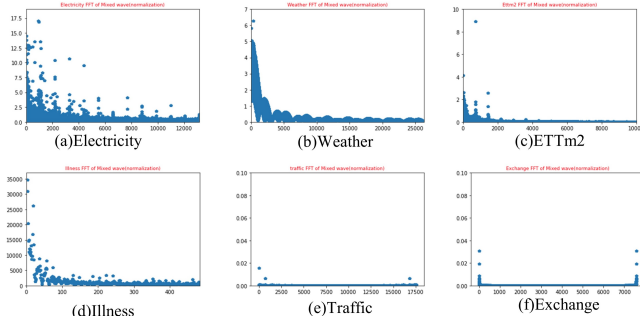


**Figure 2: six real world datasets visualization in Frequency domain, we can see most energy is contained in low frequency range.**

Some efforts has been done for getting frequency representation and reconstructing temporal signal based on Fourier Transform and it's inverse transform. However, Fourier Transform (FT) would introduce high-frequency components for its problematic periodicity, causing error value for boundary information which call Gibbs phenomenon and new round of computation consumption for inverse operation for avoiding complex operation in networks. Unlike FT/IFT based methods, Our method is based on Discrete Cosine Transform which would intrinsically eradicate Gibbs Phenomenon mentioned above and save unnecessary consumption of inverse transform, and for better exploiting utility of relationship between different time-series variate, we propose Frequency Enhanced Channel Attention Mechanism as a general framework, which empowers Transformer-based method and other mainstream models like LSTM, with better predictive ability for real-world time series. Consequently, effectively utilizing frequency information of time series enable us to perform forecasting with reasonable accuracy. Our method achieves state-of-the-art performance on six

real-world benchmarks as a model. Furthermore, as a module FECAM can generalize to various Networks for further improvement, with just few line codes.

To this end, we propose a general feature extraction method for sequence modeling and forecasting, named frequency enhanced channel attention mechanism, which intrinsically eradicate Gibbs Phenomenon caused by Fourier Transform for the first time in time series forecasting. Our method achieves state-of-the-art performance on six real-world datasets, and can be generalized to other model architectures with just few line codes. The contributions of this paper are summarized as follows:

- We theoretically prove that our method can mitigate Gibbs phenomenon which would introduce high frequency noise during Fourier Transform, and we demonstrate that GAP is the lowest frequency component of DCT.
- Based on above proof, We build the channel attention in frequency domain and propose our method with frequency enhanced channel mechanism for time-series forecasting. For generalization, we generalize frequency-enhanced channel attention into module that can be easily and flexibly adapted into other mainstream time series forecasting models to get better performance on six real-world datasets.
- Extensive experiments on various TSF datasets show that FECAM as a general method consistently boosts four mainstream Transformers and non-transformer based methods like LSTM by a considerable margin and achieves state-of-the-art performance on six real-world datasets.

## 2 RELATED WORK AND PRELIMINARY

### 2.1 Deep Learning Models for Times series forecasting

In recent years, deep learning models with meticulously designed architectures have achieved excellent progress in TSF tasks. RNN-based models [25, 29, 33, 38, 43] are proposed for application in an auto-regressive manner for sequence modeling, but the recurrent structure can suffer from problem of modeling long-term dependency. Shortly afterwards, Transformer [35] emerges and shows great power in sequence modeling and gains great achievements in various downstream tasks. To solve the quadratic computation consumption on sequence length, subsequent works aim to decrease Self-Attention's complexity. Particularly in long-term time

series forecasting, Informer [47] extends Self-Attention with KL-divergence criterion to select dominant queries. Reformer [18] introduces local-sensitive hashing (LSH) mechanism to approximate attention by allocated similar queries. Not just improvement of reduction complexity, the following models further develop delicate building blocks for time series forecasting. Autoformer [40] coalesce the decomposition blocks into a canonical structure and designs Auto-Correlation to capture series-wise connections. Pyraformer [22] designs pyramid attention module (PAM) to capture temporal dependencies with different hierarchies. Transformer-based models have taken the place of RNN-based models in almost all sequence modeling tasks, thanks to the effectiveness and efficiency of the self-attention mechanisms. Various Transformer-based TSF methods are proposed in the literature. These works typically focus on the challenging long-term time series forecasting problem, taking advantage of their remarkable long sequence modeling capabilities.

Although the transformers can capture long-range dependency in the time domain, it does not explicitly model the pattern occurrences in the frequency domain that plays an important role in tracking and predicting data points over various time cycles.

Different from previous works focusing on architectural design based on transformers, we analyze the series forecasting task from the natural view of frequency, which is the essential property of time series. It is also notable that as a general block, our proposed frequency-enhanced channel block can be easily applied to various models with a few operation. In the following subsection, we highlight our insights and motivate our work.

## 2.2 Frequency Representation for time series forecasting

Frequency is an indispensable information of time series, and real world datasets often contain rich frequency information as shown in Fig.2, which allows better utilization of the capabilities of deep learning models. To utilize frequency information, Auto-former [40] use FFT in efficient computing of auto-correlation function, FNO [14] is used as an inner block of networks to perform representation learning in low-frequency domain, DCTnet [42] use Discrete Cosine Transform to compress information for keeping more original picture information in CV task. Most of these work was based on Fourier Transform which is helpful for extracting frequency features. However, most of the FT-based methods use Fourier Transform to get the frequency information and use Inverse Fourier Transform to reconstruct temporal information for avoiding complex-number training, which introduces new amount of computation, which is avoidable if using DCT for time-frequency transformation, what's more the implicit periodicity of DFT gives rise to boundary discontinuity that result in significant high-frequency content which is known as Gibbson Phenomeneon. After quantization, Gibbs Phenomeneon causes the boundary points to take on erraneous values. SENET [15] only use GAP which is the lowest component of DFT and DCT for channel representation, meaning discarding other frequency-component information.

## 2.3 Problem of Gibbs Phenomenon

The Gibbs phenomenon [9, 26, 34] involves both the fact that Fourier sums overshoot at a jump discontinuity, and that this overshoot

does not die out as more sinusoidal terms are added. And this would cause high frequencies noise which is supposed to be avoidable for time series forecasting. We demonstrate the phenomenon for square wave (In Fig.3) with the additive synthesis of a square wave with an increasing number of harmonics. The Gibbs phenomenon is visible especially when the number of harmonics is large. We give the mathematic description of Gibbs Phenomenon below.

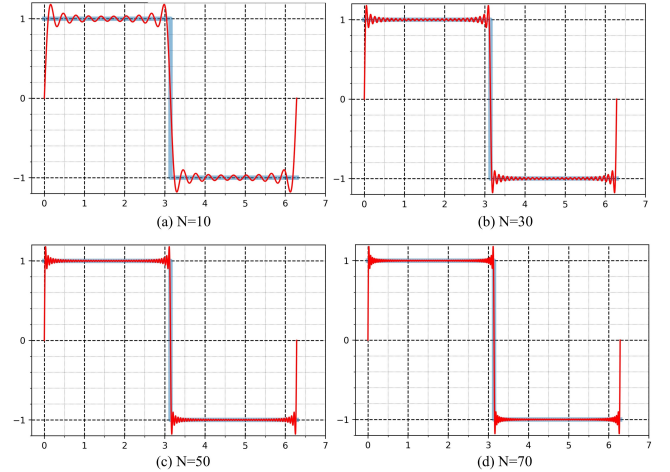


**Figure 3: Gibbs Phenomenon with increasing harmonics component.**

**Formal mathematical description of the phenomenon:** Let  $f : \mathbb{R} \rightarrow \mathbb{R}$  be a piecewise continuously differentiable function which is periodic with some period  $L > 0$ . Suppose that at some point  $x_0$ , the left limit  $f(x_0^-)$  and right limit  $f(x_0^+)$  of the function  $f$  differ by a non-zero jump of  $a$ :

$$f(x_0^+) - f(x_0^-) = a \neq 0. \quad (1)$$

For each positive integer  $N$ , let  $S_N f(x)$  be the  $N$ th partial Fourier series

$$\begin{aligned} S_N f(x) &:= \sum_{-N \leq n \leq N} \widehat{f}(n) e^{\frac{2i\pi nx}{L}} \\ &= \frac{1}{2} a_0 + \sum_{n=1}^N \left( a_n \cos\left(\frac{2\pi nx}{L}\right) + b_n \sin\left(\frac{2\pi nx}{L}\right) \right), \end{aligned} \quad (2)$$

where the Fourier coefficients  $\widehat{f}(n)$ ,  $a_n$ ,  $b_n$  are given by the usual formulae

$$\begin{aligned} \widehat{f}(n) &:= \frac{1}{L} \int_0^L f(x) e^{-2i\pi nx/L} dx \\ a_n &:= \frac{2}{L} \int_0^L f(x) \cos\left(\frac{2\pi nx}{L}\right) dx \\ b_n &:= \frac{2}{L} \int_0^L f(x) \sin\left(\frac{2\pi nx}{L}\right) dx. \end{aligned} \quad (3)$$

Then we have:

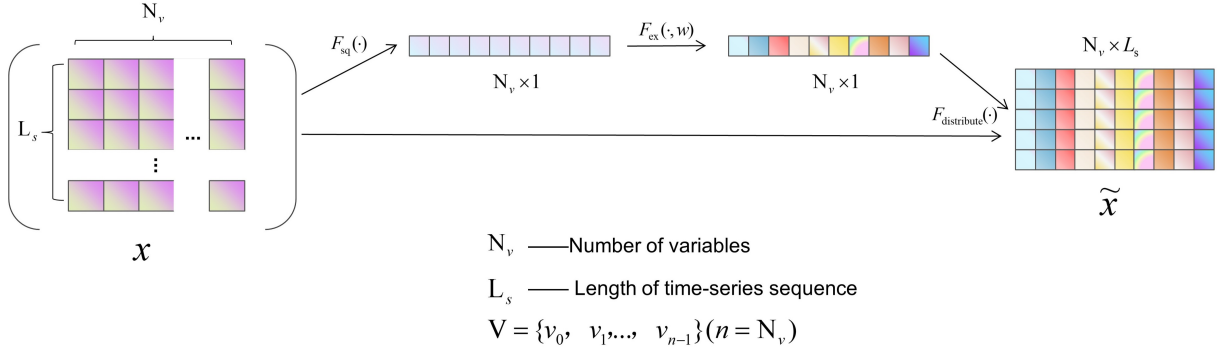


Figure 4: SENET channel attention(Squeeze and excitation Network),  $F_{sq}(\cdot)$  represent usg1d-global average pooling to extract global information a full connected layer for from channel and redistribute weight for each channel.

$$\lim_{N \rightarrow \infty} S_N f \left( x_0 + \frac{L}{2N} \right) = f(x_0^+) + a \cdot (0.089489872236 \dots) \quad (4)$$

and

$$\lim_{N \rightarrow \infty} S_N f \left( x_0 - \frac{L}{2N} \right) = f(x_0^-) - a \cdot (0.089489872236 \dots) \quad (5)$$

but

$$\lim_{N \rightarrow \infty} S_N f(x_0) = \frac{f(x_0^-) + f(x_0^+)}{2}. \quad (6)$$

More generally, if  $x_N$  is any sequence of real numbers which converges to  $x_0$  as  $N \rightarrow \infty$ , and if the jump of  $a$  is positive then

$$\limsup_{N \rightarrow \infty} S_N f(x_N) \leq f(x_0^+) + a \cdot (0.089489872236 \dots) \quad (7)$$

and

$$\liminf_{N \rightarrow \infty} S_N f(x_N) \geq f(x_0^-) - a \cdot (0.089489872236 \dots) \quad (8)$$

If instead the jump of  $a$  is negative, one needs to interchange limit superior with limit inferior, and also interchange the  $\leq$  and  $\geq$  signs, in the above two inequalities.

### 3 FECAM: FREQUENCY ENHANCED CHANNEL ATTENTION MECHANISM

Frequency is a natural auxiliary means to analyze time series. It is important and intuitive to introduce frequency information into time series models. However, most time series models tend to ignore the impact of frequency information on time series tasks, resulting in failure to learn the inherent characteristics of time series information. Most methods of extracting frequency information are based on FT and IFT, However, methods based on FT and IFT tends to introduce high-frequency noise due to problematic periodicity which is known as Gibbs Phenomenon, Frequency Enhanced Frequency Channel Attention Mechanism can intrinsically avoid problem mentioned above and automatically acquire the importance of each channel through learning, it also suppresses features that are not useful for the current task.

We expect the learning of channel interdependencies features to be enhanced by explicitly modelling in frequency domain.

#### 3.1 Channel Attention and DCT

We first elaborate on the definitions of discrete cosine transform and channel attention mechanism.

**3.1.1 Revisiting Channel attention.** The channel attention mechanism has been successfully introduced to CNNs. Squeeze-and-excitation (SE) block [15] models the interdependencies between the channels of feature maps with global information and recalibrate the feature maps to improve representation ability. It consists of squeeze and excitation two steps which are depicted in Fig. 4. For time-series signals  $X \in R^{C \times L}$ ,  $C$  is the number of channels,  $L$  is the length of the temporal sequence, this type of tensor could be anywhere in the time-series model.

For temporal signals, the squeeze step applies GAP on temporal dimension to generate channel wise descriptor. Officially, a statistic  $Z_c \in R^c$  is generated by shrinking  $x$  through its temporal dimension  $L_s$ , such that the  $c$ -th item of  $z$  is calculated by:

$$Z_c = GAP(x_c) = \frac{1}{L_s} \sum_{i=1}^{L_s} x_c(i) \quad (9)$$

Where  $c, L_s$  represent the channel, and temporal dimension respectively. The scalar  $Z_c$  is the  $c$ -th element of  $Z$ , Then the excitation step aims to modelling channel-wise dependencies by using two fully-connected layers  $W_1$  and  $W_2$  with a bottleneck architecture and non-linearity:

$$att = \sigma(W_2 \delta(W_1 Z)) \quad (10)$$

where  $att \in R^C$  is the learned attention vector which dot multiplies to the original feature map to re-scale each channel,  $\sigma$  and  $\delta$  refer to ReLU and sigmoid activation function respectively.

**3.1.2 Frequency representation for time series.** Sometimes, frequency information contains more information that can be found, but it is difficult to mine in the time domain. For example, when a signal is disturbed by noise, its waveform will become messy, Or we can't distinguish it from noise in time domain. But it can be clearly distinguished from the frequency domain. Instead of well-known Fourier Transform, Our method introduce frequency information

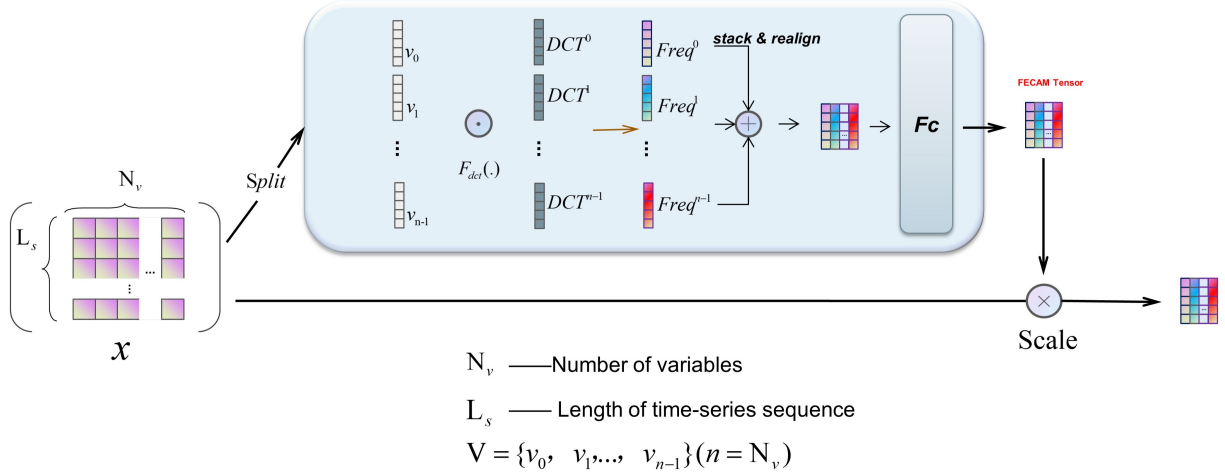


**Figure 5: Structure of Frequency Enhanced Channel Attention Mechanism. split every sequence of multivariate time series in each channel and Fdet(.) stands for Discrete Cosine Transform, stack&realign each channel together.**

by Discrete Cosine Transform which can intrinsically avoid G-phenomenon and inverse transform operation.

#### Discrete Cosine Transform (DCT)

Typically, the basis function of one-dimensional (1D) DCT is:

$$B_l^i = \cos\left(\frac{\pi l}{L_s}\left(i + \frac{1}{2}\right)\right) \quad (11)$$

Then the 1D DCT can be written as:

$$f_{1d}^l = \sum_{i=0}^{L_s-1} x_i^{1d} B_l^i \quad (12)$$

s.t.  $l \in \{0, 1, \dots, L_s - 1\}$ , In which  $f_{1d}^l \in R^L$  is the 1D DCT frequency spectrum,  $x^{1d} \in R^L$  is the input,  $L$  is the length of  $x^{1d}$ . Correspondingly, the inverse 1D DCT can be written as:

$$x_i^{1d} = \sum_{l=0}^{L_s-1} f_{1d}^l B_l^i \quad (13)$$

s.t.  $i \in \{0, 1, \dots, L_s - 1\}$ , In which  $f_{1d}^l \in R^L$ , Please note that in Eqs. 2 and 3, some constant normalization factors are removed for simplicity, which will not affect the results in this work.

### 3.2 Frequency Enhanced Channel Attention Mechanism

In this section, we first theoretically discuss the problem of existing channel attention mechanisms. Based on the theoretical analysis, we then elaborate on the network design of the proposed method.

Although GAP is a widely used operation in many attention mechanism as a standard squeezing method, we argue that simply use average-pooling on temporal dimension cause inadequate information extraction from time series which would even leads to information loss. Since GAP is the lowest frequency component of DCT and DFT, we mitigate this problem by introducing more frequency information. Rather than DFT, We use DCT to evade the Gibbs phenomenon mentioned many times before.

**Theorem 1.** *1d-GAP is a lowest component of 1D DCT, and its result is proportional to the lowest frequency component of 1d-DCT.*

$$f_0^{1d} = \sum_{i=0}^{L_s-1} x_i^{1d} \cos\left(\frac{0}{L_s}\left(i + \frac{1}{2}\right)\right) = \sum_{i=0}^{L_s-1} x_i^{1d} = \text{gap}(x^{1d})_{L_s} \quad (14)$$

In Eq.14,  $f_0^{1d}$  represents the lowest frequency component of 1D DCT, and it is proportional to GAP. In this way, Theorem 1 is proved.

According to Theorem 1, without any surprise, we can sure that using GAP for feature extraction in channel attention means only the lowest frequency in obtained. All other frequency components are ignored, which supposed to be included in presenting channels.

**Theorem 2.** *Discrete Cosine Transform can intrinsically avoid Gibbs Phenomenon caused by periodic problem of Discrete Fourier Transform and Inverse Discrete Fourier Transform, and have a more efficient energy compaction than Fourier Transform.*

Discrete Cosine Transform is actually the DFT whose input signal is a real even function (proved in Derivation of DCT in Appendix A). Since Discrete Cosine Transform is using symmetric expansion for it's periodic extension (In Fig.6). Therefore, followed with eq.1, we have:

$$f(x_0^+) - f(x_0^-) = a = 0 = f(x_0) \Leftrightarrow f(x_0^+) = f(x_0^-) \quad (15)$$

Equation 15 means that there's no jump discontinuity which is necessary condition of Gibbs Phenomenon.

Then follow with eq.4 and eq.5, then we have:

$$\lim_{N \rightarrow \infty} S_N f\left(x_0 + \frac{L}{2N}\right) = f(x_0^+) + 0 \cdot (0.0894 \dots) \quad (16)$$

$$\lim_{N \rightarrow \infty} S_N f\left(x_0 - \frac{L}{2N}\right) = f(x_0^-) - 0 \cdot (0.0894 \dots) \quad (17)$$

Follow with eq.7 and eq.8,

$$\Rightarrow \lim_{N \rightarrow \infty} \text{Sup} S_N f(x_0) \leq f(x_0^+) \quad (18)$$



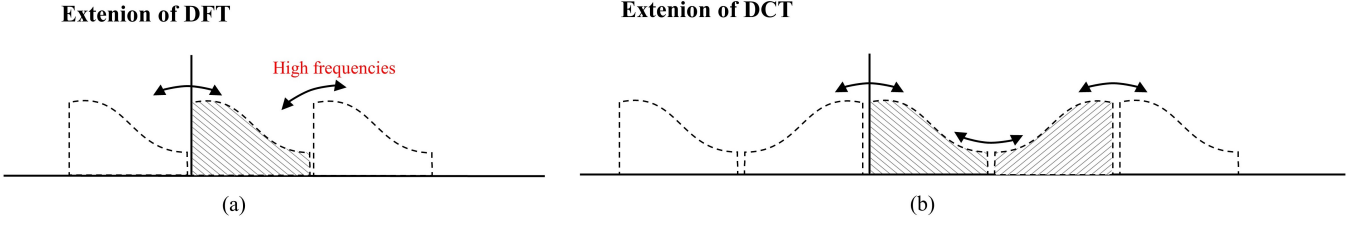


Figure 6: Extension of Discrete Fourier Transform and Discrete Cosine Transform.

$$\Rightarrow \lim_{N \rightarrow \infty} \text{Inf } S_N f(x_0) \geq f(x_0^-) \quad (19)$$

$$\lim_{N \rightarrow \infty} S_N f(x_0) = \frac{f(x_0^+) + f(x_0^-)}{2} = f(x_0) \quad (20)$$

As we can see, the limit of the formula converges at this point, no oscillation observed, thus fundamentally eliminating the Gibbs effect. Because IFT and FT is consistent in mathematical nature, it is also true for the inverse DFT. It's worthy to note that in the DFT case the periodic extension introduces discontinuities, which not happen for the DCT due to its property of symmetry extension, it is the elimination of this artificial discontinuity which contains a lot of high frequencies make the DCT is much more energy efficient than Discrete Fourier Transform. To this extent, Theorem 2 is proved. And we have done experiments to validate our Theorem 2 in section 4.4.

According to Theorem 2, we can found that in the DFT case the extension introduces discontinuities and this does not happen for DCT, due to the symmetry of its periodic extension, then our method eliminate this artificial discontinuity which contains a lot of high frequencies.

For capturing more time series information from feature map, we try to introduce DCT for getting more frequency components instead of only the GAP for lowest frequency [15]. Since DCT weight are constant, it can be pre-calculated only once and saved in advance, what's more, results are real number, which means no training time for inverse transform and number of network parameters. Therefore, we propose frequency enhanced channel attention mechanism (FECAM) which can not only be used as a model for forecasting with just adding a projection layer but also can be seamlessly added to the existing time series forecasting models for improving their prediction performance. The overall structure of FECAM is shown in Fig.5.

First, FECAM splits the input feature maps along the channel dimension into  $n$  sub-groups as  $[v_0, v_1, \dots, v_{n-1}]$ , in which  $V^i = R^{1 \times L}$ ,  $i \in \{0, 1, \dots, n-1\}$ ,  $n = N_v$ . Subsequently, for sub-group will be processed by a corresponding DCT frequency component ranging from low frequency to high frequency, Every single channel will be processed by the same frequency component, In this way we have:

$$Freq^i = DCT_j(V^i) = \sum_{j=0}^{L_S-1} (V_{:,l}^i) B_l^j \quad (21)$$

s.t.  $i \in \{0, 1, \dots, N_V - 1\}$ ,  $j \in \{0, 1, \dots, L_S - 1\}$ , in which  $j$  are the frequency component 1D indices corresponding to  $V^i$ , and  $Freq^i \in R^L$  is the  $L$  dimensional vector after the discrete cosine

transformation. The whole frequency channel vector can be obtained by stack operation.

$$Freq = DCT(V) = \text{stack}([Freq^0, Freq^1, \dots, Freq^{n-1}]) \quad (22)$$

In which  $Freq \in R^{C \times L}$  is the attention vector for  $V \in R^{C \times L}$ . Once we obtain  $Freq$ , the attention weight can be learned through neural structure as SE-block. The whole frequency enhanced channel attention mechanism framework can be written as:

$$F_c - att = \sigma(W_2 \delta(W_1 DCT(V))) \quad (23)$$

By doing so, each channel features interact with every frequency components to acquire important temporal information comprehensively from frequency domain, which would encourages networks to enhance the diversity of extracted features. In the subsequent experiment section 4.3, we visualize the frequency channel attention tensor Fig.10, demonstrating that FECAM learned the importance of different channels in the frequency domain and the importance of different frequency component pairs in each channel.

## 4 EXPERIMENTS

We conduct extensive experiments to evaluate the performance of frequency enhanced channel mechanism network on six real-world time series forecasting benchmarks and further validate the generality of the proposed method on various mainstream Transformer variants and non-transformer based models. As a module embedding to other Networks, we have also done experiment of parameters increment and performance promotion and the visualization of frequency channel attention tensor to prove proposed method's effectiveness and efficiency.

**Datasets:** Here are the descriptions of the datasets:

**Electricity**<sup>1</sup>: records the hourly electricity consumption of 321 clients from 2012 to 2014.

**ETT**<sup>2</sup>: contains the time series of oil temperature and power load collected by electricity transformers from July 2016 to July 2018. ETTm1/ETTm2 are recorded every 15 minutes, and ETTh1/ETTh2 are recorded every hour.

**Exchange**<sup>3</sup>: collects the panel data of daily exchange rates from 8 countries from 1990 to 2016.

<sup>1</sup>The Electricity dataset was acquired at <https://archive.ics.uci.edu/ml/datasets/ElectricityLoadDiagrams20112014>

<sup>2</sup>The ETT dataset was acquired at <https://github.com/zhouhaoyi/ETDataset>

<sup>3</sup>The Exchange dataset was acquired at <https://github.com/thuml/Autoformer>

**Table 1: Statistics of datasets.**

Dataset	Variable Number	Sampling Frequency	Total Observations
Exchange	8	1 Day	7,588
ILI	7	1 Week	966
ETTM2	7	15 Minutes	69,680
Electricity	321	1 Hour	26,304
Traffic	862	1 Hour	17,544
Weather	21	10 Minutes	52,695

**Table 2: Forecasting results comparison under different prediction lengths  $O \in \{96, 192, 336, 720\}$ . The input sequence length is set to 36 for ILI and 96 for the others.**

Models		Ours		Autoformer		Pyraformer		Informer		LogTrans		Reformer		LSTNet	
Metric		MSE	MAE	MSE	MAE	MSE	MAE	MSE	MAE	MSE	MAE	MSE	MAE	MSE	MAE
Exchange	96	<b>0.085</b>	<b>0.208</b>	0.197	0.323	0.852	0.780	0.847	0.752	0.968	0.812	1.065	0.829	1.551	1.058
	192	<b>0.210</b>	<b>0.338</b>	0.300	0.369	0.993	0.858	1.204	0.895	1.04	0.851	1.610	1.020	1.477	1.028
	336	<b>0.344</b>	<b>0.445</b>	0.509	0.524	1.240	0.958	1.672	1.036	1.659	1.081	2.226	1.192	1.507	1.031
	720	<b>0.921</b>	<b>0.717</b>	1.447	0.941	1.711	1.093	2.478	1.31	1.941	1.127	1.802	1.131	2.285	1.243
ILI	24	<b>2.101</b>	<b>0.939</b>	3.483	1.287	5.800	1.693	5.764	1.677	4.475	1.444	4.400	1.382	6.026	1.770
	36	<b>2.330</b>	<b>0.951</b>	3.103	1.148	6.043	1.733	4.755	1.467	4.799	1.467	4.783	1.448	5.340	1.668
	48	<b>2.557</b>	<b>1.061</b>	2.669	1.085	6.213	1.763	4.763	1.469	4.800	1.468	4.832	1.465	6.080	1.787
	60	<b>2.531</b>	<b>1.093</b>	2.770	1.125	6.531	1.814	5.264	1.564	5.278	1.560	4.882	1.483	5.548	1.720
ETTM2	96	<b>0.188</b>	<b>0.275</b>	0.255	0.339	0.409	0.479	0.365	0.453	0.768	0.642	0.658	0.619	3.142	1.365
	192	<b>0.265</b>	<b>0.336</b>	0.281	0.340	0.673	0.641	0.533	0.563	0.989	0.757	1.078	0.827	3.154	1.369
	336	<b>0.318</b>	<b>0.362</b>	0.339	0.372	1.210	0.846	1.363	0.887	1.334	0.872	1.549	0.972	3.160	1.369
	720	<b>0.416</b>	<b>0.417</b>	0.422	0.419	4.044	1.526	3.379	1.388	3.048	1.328	2.631	1.242	3.171	1.368
Electricity	96	<b>0.178</b>	<b>0.267</b>	0.201	0.317	0.498	0.299	0.274	0.368	0.258	0.357	0.312	0.402	0.680	0.645
	192	<b>0.185</b>	<b>0.273</b>	0.222	0.334	0.828	0.312	0.296	0.386	0.266	0.368	0.348	0.433	0.725	0.676
	336	<b>0.199</b>	<b>0.290</b>	0.231	0.338	1.476	0.326	0.300	0.394	0.280	0.380	0.350	0.433	0.828	0.727
	720	<b>0.235</b>	<b>0.323</b>	0.254	0.361	4.090	0.372	0.373	0.439	0.283	0.376	0.340	0.420	0.957	0.811
Traffic	96	<b>0.493</b>	<b>0.318</b>	0.613	0.388	0.684	0.393	0.719	0.391	0.684	0.384	0.732	0.423	1.107	0.685
	192	<b>0.496</b>	<b>0.319</b>	0.616	0.382	0.692	0.394	0.696	0.379	0.685	0.390	0.733	0.420	1.157	0.706
	336	<b>0.511</b>	<b>0.325</b>	0.622	0.337	0.699	0.396	0.777	0.420	0.733	0.408	0.742	0.420	1.216	0.730
	720	<b>0.547</b>	<b>0.343</b>	0.660	0.408	0.712	0.404	0.864	0.472	0.717	0.396	0.755	0.423	1.481	0.805
Weather	96	<b>0.182</b>	<b>0.242</b>	0.266	0.336	0.354	0.392	0.300	0.384	0.458	0.490	0.689	0.596	0.594	0.587
	192	<b>0.223</b>	<b>0.281</b>	0.307	0.367	0.673	0.597	0.598	0.544	0.658	0.589	0.752	0.638	0.560	0.565
	336	<b>0.270</b>	<b>0.320</b>	0.359	0.395	0.634	0.592	0.578	0.523	0.797	0.652	0.639	0.596	0.597	0.587
	720	<b>0.338</b>	<b>0.374</b>	0.419	0.428	0.942	0.723	1.059	0.741	0.869	0.675	1.130	0.792	0.618	0.599

**ILI**<sup>4</sup>: collects the ratio of influenza-like illness patients versus the total patients in one week, which is reported weekly by Centers for Disease Control and Prevention of the United States from 2002 and 2021.

**Traffic**<sup>5</sup>: contains hourly road occupancy rates measured by 862 sensors on San Francisco Bay area freeways from January 2015 to December 2016.

**Weather**<sup>6</sup>: includes meteorological time series with 21 weather indicators collected every 10 minutes from the Weather Station of the Max Planck Biogeochemistry Institute in 2020.

<sup>4</sup>The ILI dataset was acquired at <https://gis.cdc.gov/grasp/fluview/fluportaldashboard.html>

<sup>5</sup>The Traffic dataset was acquired at <http://pems.dot.ca.gov/>

<sup>6</sup>The Weather dataset was acquired at <https://www.bgc-jena.mpg.de/wetter/>

**Table 3: Univariate results with different prediction lengths  $O \in \{96, 192, 336, 720\}$  on datasets ETTm2 and Exchange. The input sequence length is set to 96.**

Models		Ours		N-HiTs		N-BEATS		Autoformer		Pyraformer		Informer		Reformer		ARIMA	
Metric		MSE	MAE	MSE	MAE	MSE	MAE	MSE	MAE	MSE	MAE	MSE	MAE	MSE	MAE	MSE	MAE
Exchange	96	<b>0.085</b>	<b>0.208</b>	0.114	0.248	0.156	0.299	0.241	0.387	0.290	0.439	0.591	0.615	1.327	0.944	0.112	0.245
	192	<b>0.206</b>	<b>0.338</b>	0.250	0.387	0.669	0.665	0.273	0.403	0.594	0.644	1.183	0.912	1.258	0.924	0.304	0.404
	336	<b>0.344</b>	<b>0.445</b>	0.434	0.516	0.611	0.605	0.508	0.539	0.962	0.824	1.367	0.984	2.179	1.296	0.736	0.598
	720	<b>0.759</b>	<b>0.672</b>	1.061	0.773	1.111	0.860	0.991	0.768	1.285	0.958	1.872	1.072	1.280	0.953	1.871	0.935
ETTM2	96	0.066	<b>0.188</b>	0.092	0.232	0.082	0.219	<b>0.065</b>	0.189	0.074	0.208	0.088	0.225	0.131	0.288	0.211	0.362
	192	<b>0.109</b>	<b>0.245</b>	0.128	0.276	0.120	0.268	0.118	0.256	0.116	0.252	0.132	0.283	0.186	0.354	0.261	0.406
	336	<b>0.144</b>	<b>0.287</b>	0.165	0.314	0.226	0.370	0.154	0.305	0.143	0.295	0.180	0.336	0.220	0.381	0.317	0.447
	720	<b>0.177</b>	<b>0.326</b>	0.243	0.397	0.188	0.338	0.182	0.335	0.197	0.338	0.300	0.435	0.267	0.430	0.366	0.487

Table 1 summarizes overall statistics of the datasets. We follow the standard protocol that divides each dataset into the training, validation, and testing subsets according to the chronological order. The split ratio is 3:1:1 for the ETT dataset and 7:2:2 for others.

**Baselines:** We evaluate the single full-connected layer equipped by the Frequency Enhanced Channel Attention mechanism in both multivariate and uni-variate settings to demonstrate its effectiveness. For multivariate forecasting, we include six state-of-the-art deep forecasting models: Autoformer [40], Pyraformer [22], Informer [47], LogTrans [20], Reformer [18] and LSTMNet [19]. For univariate forecasting, we include seven competitive baselines: N-HiTs [4], N-BEATS [27], Autoformer [40], Pyraformer [22], Informer [47], Reformer [18] and ARIMA [1]. In addition, we adopt the proposed framework on both the canonical and efficient variants of Transformers and classical RNNs: Transformer [35], Informer [47], Reformer [18] and Autoformer [40] and LSTM [12] to validate the generality of our framework.

**Implementation details:** All the experiments are implemented in PyTorch [28] and conducted for three runs on a single NVIDIA GeForce RTX 3090 24GB GPU. Each model is trained by ADAM [17] using L2 loss with the initial learning rate of  $10e-4$  and batch size of 32. Each Transformer-based model contains two encoder layers and one decoder layer. We report the test MSE/MAE under different prediction lengths as the performance metric. A lower MSE/MAE indicates better performance of time series forecasting.

## 4.1 Main Results

**Forecasting results:** As for multivariate forecasting results, Our proposed method with a projection layer for forecasting achieves state-of-the-art performance in all benchmarks and prediction lengths (Table 2). Notably, Frequency Enhanced Channel Attention Mechanism outperforms other deep models impressively characterized by much less model parameters. Compared with Autoformer, the proposed FECAM yields an **overall 21.52%** relative MSE reduction and relative **10.78%** MAE reduction. With the prediction length of 24 and 48, FECAM achieve an **39.67%** MSE reduction ( $3.483 \rightarrow 2.101$ )

and **24.9%** ( $3.103 \rightarrow 2.330$ ) respectively on ILI, with the prediction length of 96, 192, 336, 720, FECAM achieve **36.40%** relative MSE on Exchange compared to previous state-of-the-art results, which indicates that the potential of deep model is still constrained on ability of modelling in frequency domain. We also list the univariate results of two typical datasets with different frequency distribution (as shown in Fig.2). FECAM still realizes remarkable forecasting performance.

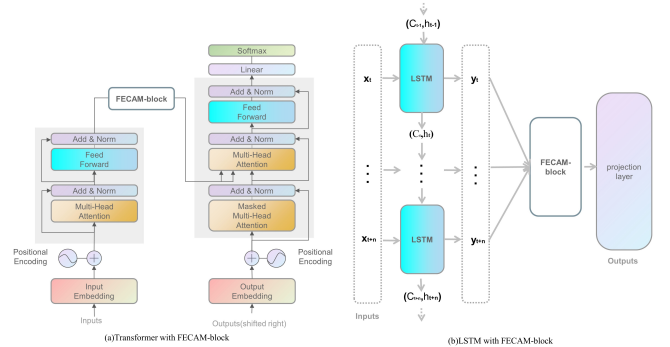


**Figure 7: FECAM as a module embedded into other Networks, figure (a) represent module is put behind the encoder of Transformers and figure (b) represent module is put between LSTM output layer and projection layer.**

**Module generality:** We apply our proposed method to four mainstream Transformers (as shown in Fig.7(a)) and a mainstream recurrent neural network LSTM (as shown in Fig.7(b)) and report the performance promotion of each model (Table 5). Our method consistently improves the forecasting ability of different models. Overall, it achieves averaged 35.99% promotion on LSTM, 10.01% on Reformer, 8.71% on Informer, 8.29% on Autoformer and 8.06% on Transformer, making each of them surpass previous state-of-the-art. Compared to vanilla models, only a few parameters are increased by applying our method (See Table 4), and thereby their computational complexities can be preserved. It validates that Frequency Enhanced



**Table 4: Parameters increment and performance promotion of FECAM**

Models	LSTM	Reformer	Informer	Autoformer	Transformer
Vanilla	13.2K	5.79MB	11.33MB	10.54MB	10.54MB
Vanilla+Ours	13.5K	5.85MB	11.39MB	10.69MB	10.60MB
Parameters increment	<b>2.27%</b>	<b>1.03%</b>	<b>0.53%</b>	<b>0.57%</b>	<b>0.57%</b>
Performance promotion	<b>35.99%</b>	<b>10.01%</b>	<b>8.71%</b>	<b>8.29%</b>	<b>8.06%</b>

**Table 5: Performance promotion by applying our proposed method method to Transformers and RNNs. We report the averaged MSE/MAE of all prediction length (stated in Table 2) and the relative MSE reduction ratios(Promotion) by our method. Complete results can be found in Appendix B**

Dataset	Exchange		ILI		ETTm2		Electricity		Traffic		Weather	
	MSE	MAE	MSE	MAE	MSE	MAE	MSE	MAE	MSE	MAE	MSE	MAE
LSTM	2.104	1.221	6.537	1.828	2.394	1.177	0.559	0.549	1.010	0.541	0.443	0.453
<b>+Ours</b>	1.294	0.946	4.305	1.442	1.338	0.896	0.381	0.437	0.755	0.430	0.277	0.333
promotion	<b>38.49%</b>		<b>34.14%</b>		<b>44.11%</b>		<b>31.84%</b>		<b>25.24%</b>		<b>37.47%</b>	
Transformer	1.556	0.969	4.774	0.445	1.344	0.814	0.272	0.367	0.667	0.363	0.681	0.576
<b>+Ours</b>	1.271	0.874	4.471	1.394	1.254	0.806	0.256	0.364	0.662	0.359	0.615	0.537
promotion	<b>18.31%</b>		<b>6.77%</b>		<b>6.69%</b>		<b>5.88%</b>		<b>0.75%</b>		<b>9.69%</b>	
Informer	1.550	0.998	5.136	1.544	1.410	0.822	0.31	0.396	0.764	0.415	0.633	0.548
<b>+Ours</b>	1.433	0.949	4.676	1.453	1.249	0.794	0.288	0.38	0.736	0.399	0.576	0.511
promotion	<b>7.54%</b>		<b>8.95%</b>		<b>11.41%</b>		<b>7.09%</b>		<b>3.66%</b>		<b>10.42%</b>	
Autoformer	0.613	0.539	3.006	1.161	0.324	0.367	0.227	0.337	0.627	0.378	0.337	0.381
<b>+Ours</b>	0.504	0.499	2.738	1.108	0.315	0.359	0.217	0.326	0.616	0.367	0.318	0.368
promotion	<b>17.78%</b>		<b>8.91%</b>		<b>2.77%</b>		<b>4.40%</b>		<b>1.75%</b>		<b>5.63%</b>	
Reformer	1.620	1.023	4.724	1.445	1.479	0.915	0.337	0.422	0.740	0.421	0.802	0.655
<b>+Ours</b>	1.275	0.907	4.398	1.378	1.443	0.897	0.318	0.397	0.711	0.394	0.585	0.551
promotion	<b>21.29%</b>		<b>6.90%</b>		<b>2.43%</b>		<b>5.63%</b>		<b>3.91%</b>		<b>27.05%</b>	

Channel Attention Mechanism is an effective and lightweight tool that can be widely applied to Transformer-based models and RNNs with a few line code, and enhances their ability of modelling in frequency domain to achieve state-of-the-art performance.

By analyzing the results of Table 5, we can obviously find that the module gains of the FECAM are large in datasets Exchange, ETTm2, and weather, but small in the dataset traffic. By observing the frequency spectrum of each dataset (as shown in the Fig.2), we can safely say that datasets like Exchange, ETTm2, and Weather have a lot of energy information at low frequencies, while there is little energy information in the frequency spectrum of the Traffic dataset, and this might be the reason why the gains of FECAM module is not so profitable on the traffic dataset.

## 4.2 Model Analysis

**Qualitative results:** As shown in Fig.8, we plot the prediction results of vanilla Transformer, Transformer with our FECAM block, and Our FECAM method (FECAM with a projection layer) on Exchange dataset, and plot the prediction results of vanilla LSTM, LSTM with

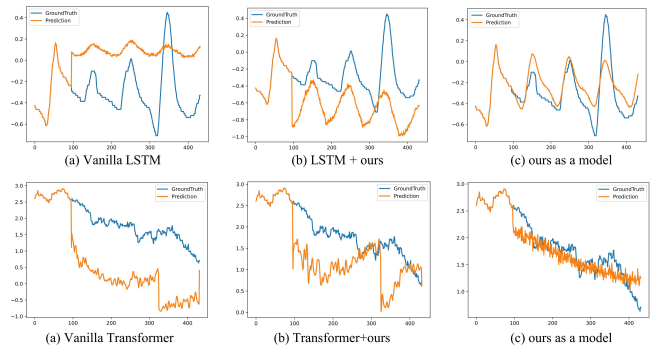


**Figure 8: Visualization of ETTm2 and Exchange predictions given by different models.**

FECAM block, and our FECAM method on ETTm2 dataset. When the input length is 96 steps and the output horizon is 336 steps, Transformer and LSTM both fail to capture the scale and bias of

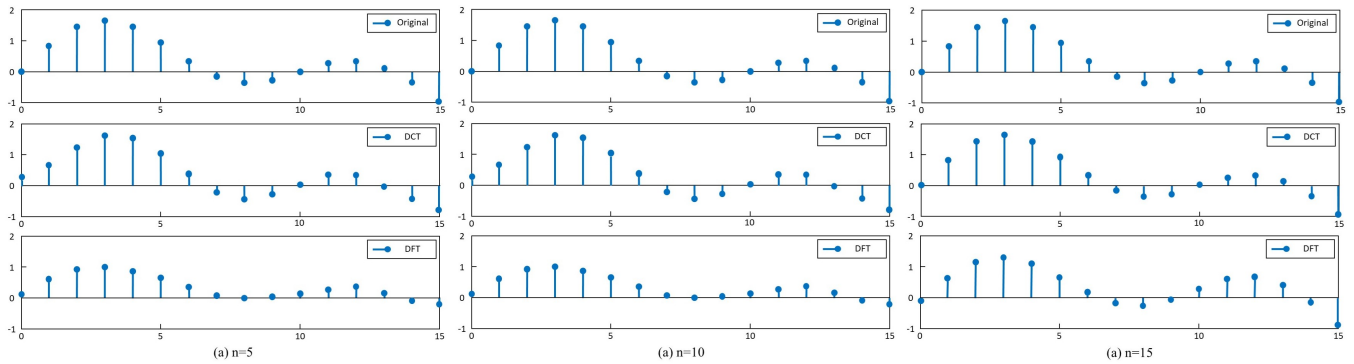


Figure 9: Signal reconstruction contrast between DCT and DFT with different number of frequency components.

the future data on Exchange and ETTm2 respectively (as shown in Fig.8(a,d)) Moreover, transformer can hardly predict a proper trend on aperiodic data such as Exchange-Rate. With Our FECAM module, both Transformer and LSTM have a better predictability compared to their vanilla version (as shown in Fig.8(b,e)). We can see FECAM with just a projection layer can have a remarkable prediction result than other models with FECAM module, it could be the reason that parameters of FECAM is much less small than Transformer and LSTM which means Transformer and LSTM are more likely to get overfitting than FECAM with just a projection layer. These phenomena further indicate the inadequacy of existing mainstream models modelling in frequency for the TSF task. Our proposed method is beneficial for an accurate prediction of the detailed series variation, which is vital in real-world time series forecasting.

### 4.3 The interpretability of FECAM

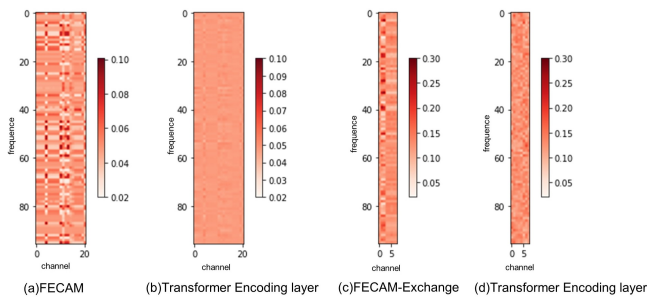


Figure 10: Visualization of frequency enhanced channel attention and output tensor of encoder layer of transformer. x-axis represents channels, y-axis represents frequency from low to high, performing on datasets weather and exchange.

Fig.10(a) and (b) visualize the tensor of channel attention in FECAM and encoder layer of Transformer on the weather dataset, and Fig.10(c) and (d) visualize the tensor of channel attention in FECAM and encoder layer of Transformer on the exchange dataset. we can see FECAM can extract the importance of different channels and the significance of different frequencies with obvious patterns compared with output tensor of encoder layer in transformer.

### 4.4 Energy Compaction

For a signal with 16 sampling points, DCT and DFT are respectively used for reconstruction. During reconstruction, DCT and DFT use  $n = \{5, 10, 15\}$  number of components starting from low frequency. The effect is as shown in Fig.9.

This experiment intuitively verified that for a signal with more energy concentrated in the low frequency, DCT can better reconstruct the signal with using less components. So Discrete Cosine Transform is more efficient in Energy compaction than Discrete Fourier Transform.

## 5 CONCLUSION

This paper addresses time series forecasting from the perspective of modelling in frequency domain. Unlike previous studies that most frequency extraction method are FT-based which could bring high-frequency noise to the results due to the problematic periodicity, which is known as Gibbs Phenomenon. We propose Frequency enhanced channel mechanism based on Discrete Cosine Transform could intrinsically avoid G-phenomenon, and we theoretically prove the feasibility of the method. By modeling in the frequency domain, FECAM can assign channel weights to different channels, and learn the importance of different frequencies of each channel, so as to learn the frequency domain representation of time series. In the experimental stage, we visualize the frequency domain information extracted by FECAM, which verify our conjecture and proved its validity. Most importantly, for its generalization, we design this method into a module for accessibility, which can flexibly and easily use in other mainstream model like transformer-based methods and RNNs methods, etc., with just a few lines to add. Our work achieve state-of-the-art on six real-world benchmarks. This impressive generality and performance of proposed frequency enhanced channel attention mechanism can be interesting of future research for time series forecasting.

## ACKNOWLEDGMENTS

This work was supported by the National Key R&D Program of China (No. 2020YFB1709702) and the National Natural Science Foundation of China (No. 62073313).

## REFERENCES

- [1] O. Anderson and M. Kendall. 1976. Time-Series. 2nd edn. *J. R. Stat. Soc. (Series D)* (1976).
- [2] Silvio Barra, Salvatore Mario Carta, Andrea Corrigan, Alessandro Sebastian Podda, and Diego Reforgiato Recupero. 2020. Deep learning and time series-to-image encoding for financial forecasting. *IEEE/CAA Journal of Automatica Sinica* 7, 3 (2020), 683–692.
- [3] Jian Cao, Zhi Li, and Jian Li. 2019. Financial time series forecasting model based on CEEMDAN and LSTM. *Physica A: Statistical mechanics and its applications* 519 (2019), 127–139.
- [4] Cristian Challu, Kin G Olivares, Boris N Oreshkin, Federico Garza, Max Mergenthaler, and Artur Dubrawski. 2022. N-HiTS: Neural Hierarchical Interpolation for Time Series Forecasting. *arXiv preprint arXiv:2201.12886* (2022).
- [5] Lili Chen, Kevin Lu, Aravind Rajeswaran, Kimin Lee, Aditya Grover, Michael Laskin, Pieter Abbeel, Aravind Srinivas, and Igor Mordatch. 2021. Decision Transformer: Reinforcement Learning via Sequence Modeling. *NeurIPS* (2021).
- [6] J. Devlin, Ming-Wei Chang, Kenton Lee, and Kristina Toutanova. 2019. BERT: Pre-training of Deep Bidirectional Transformers for Language Understanding. In *NAACL-HLT*.
- [7] Qianggang Ding, Sifan Wu, Hao Sun, Jiadong Guo, and Jian Guo. 2020. Hierarchical Multi-Scale Gaussian Transformer for Stock Movement Prediction.. In *IJCAI*. 4640–4646.
- [8] Alexey Dosovitskiy, Lucas Beyer, Alexander Kolesnikov, Dirk Weissenborn, Xiuhua Zhai, Thomas Unterthiner, Mostafa Dehghani, Matthias Minderer, Georg Heigold, Sylvain Gelly, Jakob Uszkoreit, and Neil Houlsby. 2021. An Image is Worth 16x16 Words: Transformers for Image Recognition at Scale. In *ICLR*. <https://openreview.net/forum?id=YicbFdNTTy>
- [9] J Foster and FB Richards. 1991. The Gibbs phenomenon for piecewise-linear approximation. *The American Mathematical Monthly* 98, 1 (1991), 47–49.
- [10] Marzyeh Ghassemi, Marco Pimentel, Tristan Naumann, Thomas Brennan, David Clifton, Peter Szolovits, and Mengling Feng. 2015. A multivariate timeseries modeling approach to severity of illness assessment and forecasting in ICU with sparse, heterogeneous clinical data. In *Proceedings of the AAAI conference on artificial intelligence*, Vol. 29.
- [11] Tilmann Gneiting and Adrian E Raftery. 2005. Weather forecasting with ensemble methods. *Science* 310, 5746 (2005), 248–249.
- [12] Klaus Greff, Rupesh K Srivastava, Jan Koutnik, Bas R Steunebrink, and Jürgen Schmidhuber. 2016. LSTM: A search space odyssey. *IEEE transactions on neural networks and learning systems* 28, 10 (2016), 2222–2232.
- [13] Aditya Grover, Ashish Kapoor, and Eric Horvitz. 2015. A deep hybrid model for weather forecasting. In *Proceedings of the 21th ACM SIGKDD international conference on knowledge discovery and data mining*. 379–386.
- [14] Gaurav Gupta, Xiongye Xiao, and Paul Bogdan. 2021. Multiwavelet-based Operator Learning for Differential Equations. *arXiv:2109.13459* [cs.LG]
- [15] Jie Hu, Li Shen, and Gang Sun. 2018. Squeeze-and-Excitation Networks. *IEEE Conference on Computer Vision and Pattern Recognition*.
- [16] Sasikiran Kandula, Teresa Yamana, Sen Pei, Wan Yang, Haruka Morita, and Jeffrey Shaman. 2018. Evaluation of mechanistic and statistical methods in forecasting influenza-like illness. *Journal of The Royal Society Interface* 15, 144 (2018), 20180174.
- [17] Diederik P. Kingma and Jimmy Ba. 2015. Adam: A Method for Stochastic Optimization. In *ICLR*. <http://arxiv.org/abs/1412.6980>
- [18] Nikita Kitaev, Lukasz Kaiser, and Anselm Levskaya. 2020. Reformer: The Efficient Transformer. In *ICLR*. <https://openreview.net/forum?id=rkgNkHtVb>
- [19] Guokun Lai, Wei-Cheng Chang, Yiming Yang, and Hanxiao Liu. 2018. Modeling long-and short-term temporal patterns with deep neural networks. In *SIGIR*.
- [20] Shiyang Li, Xiaoyong Jin, Yao Xuan, Xiyu Zhou, Wenhui Chen, Yu-Xiang Wang, and Xifeng Yan. 2019. Enhancing the Locality and Breaking the Memory Bottleneck of Transformer on Time Series Forecasting. In *NeurIPS*. <https://proceedings.neurips.cc/paper/2019/file/6775a0635c302542da2c32aa19d86be0-Paper.pdf>
- [21] Minhao Liu, Ailing Zeng, Muxi Chen, Zhijian Xu, Qiuxia Lai, Lingna Ma, and Qiang Xu. 2022. SCINet: Time Series Modeling and Forecasting with Sample Convolution and Interaction. *Thirty-sixth Conference on Neural Information Processing Systems (NeurIPS), 2022* (2022).
- [22] Shizhan Liu, Hang Yu, Cong Liao, Jianguo Li, Weiyao Lin, Alex X Liu, and Schahram Dustdar. 2021. Pyraformer: Low-complexity pyramidal attention for long-range time series modeling and forecasting. In *ICLR*.
- [23] Ze Liu, Yutong Lin, Yue Cao, Han Hu, Yixuan Wei, Zheng Zhang, Stephen Lin, and Baining Guo. 2021. Swin Transformer: Hierarchical Vision Transformer Using Shifted Windows. In *ICCV*.
- [24] Tao Ma, Constantinos Antoniou, and Tomer Toledo. 2020. Hybrid machine learning algorithm and statistical time series model for network-wide traffic forecast. *Transportation Research Part C: Emerging Technologies* 111 (2020), 352–372.
- [25] Danielle C Maddix, Yuyang Wang, and Alex Smola. 2018. Deep factors with gaussian processes for forecasting. *arXiv preprint arXiv:1812.00098* (2018).
- [26] E Moskona, P Petrushev, and EB Saff. 1995. The Gibbs phenomenon for bestL1-trigonometric polynomial approximation. *Constructive Approximation* 11, 3 (1995), 391–416.
- [27] Boris N Oreshkin, Dmitri Carpov, Nicolas Chapados, and Yoshua Bengio. 2019. N-BEATS: Neural basis expansion analysis for interpretable time series forecasting. *ICLR* (2019).
- [28] Adam Paszke, S. Gross, Francisco Massa, A. Lerer, James Bradbury, Gregory Chanan, Trevor Killeen, Z. Lin, N. Gimelshein, L. Antiga, Alban Desmaison, Andreas Köpf, Edward Yang, Zach DeVito, Martin Raison, Alykhan Tejani, Sasank Chilamkurthy, Benoit Steiner, Lu Fang, Junjie Bai, and Soumith Chintala. 2019. PyTorch: An Imperative Style, High-Performance Deep Learning Library. In *NeurIPS*.
- [29] Syama Sundar Rangapuram, Matthias W Seeger, Jan Gasthaus, Lorenzo Stella, Yuyang Wang, and Tim Januschowski. 2018. Deep state space models for time series forecasting. In *NeurIPS*.
- [30] Stephan Rasp, Peter D Dueben, Sebastian Scher, Jonathan A Weyn, Soukayna Moutatid, and Nils Thuerey. 2020. WeatherBench: a benchmark data set for data-driven weather forecasting. *Journal of Advances in Modeling Earth Systems* 12, 11 (2020), e2020MS002203.
- [31] Andrew G Reece, Andrew J Reagan, Katharina LM Lix, Peter Sheridan Dodds, Christopher M Danforth, and Ellen J Langer. 2017. Forecasting the onset and course of mental illness with Twitter data. *Scientific reports* 7, 1 (2017), 1–11.
- [32] Luis G Baca Ruiz, R Rueda, Manuel P Cuéllar, and MC Pegalajar. 2018. Energy consumption forecasting based on Elman neural networks with evolutive optimization. *Expert Systems with Applications* 92 (2018), 380–389.
- [33] David Salinas, Valentin Flunkert, Jan Gasthaus, and Tim Januschowski. 2020. DeepAR: Probabilistic forecasting with autoregressive recurrent networks. *Int. J. Forecast.* (2020).
- [34] Bernie D Shizgal and Jae-Hun Jung. 2003. Towards the resolution of the Gibbs phenomena. *J. Comput. Appl. Math.* 161, 1 (2003), 41–65. [https://doi.org/10.1016/S0377-0427\(03\)00500-4](https://doi.org/10.1016/S0377-0427(03)00500-4)
- [35] Ashish Vaswani, Noam Shazeer, Niki Parmar, Jakob Uszkoreit, Llion Jones, Aidan N Gomez, Lukasz Kaiser, and Illia Polosukhin. 2017. Attention is All you Need. In *NeurIPS*. <https://proceedings.neurips.cc/paper/2017/file/3f5ee243547dee91fbd053c1c4a845aa-Paper.pdf>
- [36] Huaizhi Wang, Zhenxing Lei, Xian Zhang, Bin Zhou, and Jianchun Peng. 2019. A review of deep learning for renewable energy forecasting. *Energy Conversion and Management* 198 (2019), 111799.
- [37] Nan Wei, Changjun Li, Xiaolong Peng, Fanhua Zeng, and Xinqian Lu. 2019. Conventional models and artificial intelligence-based models for energy consumption forecasting: A review. *Journal of Petroleum Science and Engineering* 181 (2019), 106187.
- [38] Ruofeng Wen, Kari Torkkola, Balakrishnan Narayanaswamy, and Dhruv Madeka. 2017. A multi-horizon quantile recurrent forecaster. *NeurIPS* (2017).
- [39] Steven Wong, Robin Walters, Lejun Jiang, Tamas G Molnar, and Rose Yu. 2020. Traffic Forecasting using Vehicle-to-Vehicle Communication and Recurrent Neural Networks. *NIPS., Dec* (2020).
- [40] Haixu Wu, Jiehui Xu, Jianmin Wang, and Mingsheng Long. 2021. Autoformer: Decomposition Transformers with Auto-Correlation for Long-Term Series Forecasting. In *NeurIPS*.
- [41] Yinjun Wu, Jingchao Ni, Wei Cheng, Bo Zong, Dongjin Song, Zhengzhang Chen, Yanchi Liu, Xuchao Zhang, Haifeng Chen, and Susan B Davidson. 2021. Dynamic Gaussian mixture based deep generative model for robust forecasting on sparse multivariate time series. In *Proceedings of the AAAI Conference on Artificial Intelligence*, Vol. 35. 651–659.
- [42] Kai Xu, Minghai Qin, Fei Sun, Yuhao Wang, Yen-Kuang Chen, and Fengbo Ren. 2020. Learning in the Frequency Domain. In *Proceedings of the IEEE/CVF Conference on Computer Vision and Pattern Recognition (CVPR)*.
- [43] Rose Yu, Stephan Zheng, Anima Anandkumar, and Yisong Yue. 2017. Long-term forecasting using tensor-train RNNs. *arXiv preprint arXiv:1711.00073* (2017).
- [44] Pengyu Zeng, Guoliang Hu, Xiaofeng Zhou, Shuai Li, Pengjie Liu, and Shurui Liu. 2022. Muformer: A long sequence time-series forecasting model based on modified multi-head attention. *Knowledge-Based Systems* 254 (2022), 109584.
- [45] Chaoyun Zhang and Paul Patras. 2018. Long-term mobile traffic forecasting using deep spatio-temporal neural networks. In *Proceedings of the Eighteenth ACM International Symposium on Mobile Ad Hoc Networking and Computing*. 231–240.
- [46] Qi Zhang, Jianlong Chang, Gaofeng Meng, Shiming Xiang, and Chunhong Pan. 2020. Spatio-temporal graph structure learning for traffic forecasting. In *Proceedings of the AAAI Conference on Artificial Intelligence*, Vol. 34. 1177–1185.
- [47] Haoyi Zhou, Shanghang Zhang, Jieqi Peng, Shuai Zhang, Jianxin Li, Hui Xiong, and Wancai Zhang. 2021. Informer: Beyond Efficient Transformer for Long Sequence Time-Series Forecasting. In *AAAI*.